THE JOURNAL OF BIOLOGICAL CHEMISTRY VOL. 290, NO. 38, pp. 23173–23187, September 18, 2015

Functional and Biochemical Characterization of Hepatitis C Virus (HCV) Particles Produced in a Humanized Liver Mouse Model*

Received for publication, May 4, 2015, and in revised form, July 28, 2015 Published, JBC Papers in Press, July 29, 2015, DOI 10.1074/jbc.M115.662999

Sara Calattini[a–f,1], Floriane Fusil[a–f], Jimmy Mancip[a–f], Viet Loan Dao Thi[a–f,2], Christelle Granier[a–f], Nicolas Gadot[g], Jean-Yves Scoazec[g], Mirjam B. Zeisel[h,i], Thomas F. Baumert[h–j], Dimitri Lavillette[a–f,3], Marlène Dreux[a–f,4,5], and François-Loïc Cosset[a–f,4,6]

From the [a]CIRI-International Center for Infectiology Research, Team EVIR (Enveloped Viruses, Vectors, and Innate Responses), Université de Lyon, 69007 Lyon, France, [b]INSERM, U1111, 69007 Lyon, France, [c]Ecole Normale Supérieure de Lyon, 69007 Lyon, France, [d]Université Lyon 1, Centre International de Recherche en Infectiologie, 69007 Lyon, France, [e]CNRS, UMR5308, 69007 Lyon, France, [f]LabEx Ecofect, Université de Lyon, 69007 Lyon, France, [g]Structure Fédérative de Recherche (SFR) Lyon-Est, ANIPATH-Centre d'Histopathologie du Petit Animal de laboratoire, CNRS UMS3453-INSERM US7, 69372 Lyon, France, [h]INSERM, U1110, Institut des Maladies Virales et Hépatiques, 67000 Strasbourg, France, [i]University of Strasbourg, 67000 Strasbourg, France, and [j]Institut Hospitalo-Universitaire, Pôle Hépato-digestif, Hôpitaux Universitaires de Strasbourg, 67000 Strasbourg, France

Background: We compared viral subpopulations derived from humanized liver mouse model *versus* cell culture.
Results: *In vivo* and *in vitro* produced particles show different biophysical properties and receptor usage.
Conclusion: *In vivo* models allow functional investigations on how lipid metabolism and hepatic environment influence HCV entry.
Significance: HCV produced from humanized liver mice may better reflect the characteristics of virus from HCV-infected patients.

Lipoprotein components are crucial factors for hepatitis C virus (HCV) assembly and entry. As hepatoma cells producing cell culture-derived HCV (HCVcc) particles are impaired in some aspects of lipoprotein metabolism, it is of upmost interest to biochemically and functionally characterize the *in vivo* produced viral particles, particularly regarding how lipoprotein components modulate HCV entry by lipid transfer receptors such as scavenger receptor BI (SR-BI). Sera from HCVcc-infected liver humanized FRG mice were separated by density gradients. Viral subpopulations, termed HCVfrg particles, were characterized for their physical properties, apolipoprotein association, and infectivity. We demonstrate that, in contrast to the widely spread distribution of apolipoproteins across the different HCVcc subpopulations, the most infectious HCVfrg particles are highly enriched in apoE, suggesting that such apolipoprotein enrichment plays a role for entry of *in vivo* derived infectious particles likely via usage of apolipoprotein receptors. Consistent with this salient feature, we further reveal previously undefined functionalities of SR-BI in promoting entry of *in vivo* produced HCV. First, unlike HCVcc, SR-BI is a particularly limiting factor for entry of HCVfrg subpopulations of very low density. Second, HCVfrg entry involves SR-BI lipid transfer activity but not its capacity to bind to the viral glycoprotein E2. In conclusion, we demonstrate that composition and biophysical properties of the different subpopulations of *in vivo* produced HCVfrg particles modulate their levels of infectivity and receptor usage, hereby featuring divergences with *in vitro* produced HCVcc particles and highlighting the powerfulness of this *in vivo* model for the functional study of the interplay between HCV and liver components.

To complete its life cycle and to produce new infectious particles, HCV[7] hijacks the host lipid metabolism. Indeed, it has been demonstrated that HCV assembly is tightly connected to the assembly pathway of very low density lipoprotein (VLDL). In the most considered assembly model, the nascent nucleocapsids fuse with VLDL precursors during the VLDL maturation process across the endoplasmic reticulum membranes. Before leaving the cells, these lipoproteins acquire lipids and

* This work was supported in part by the French "Agence Nationale de la Recherche sur le SIDA et les hépatites virales" (ANRS), "ANRS consortium on humanized mouse models for viral hepatitis," the FINOVI foundation, European Research Council Grant ERC-2008-AdG-233130-HEPCENT, and LabEx Ecofect Grant ANR-11-LABX-0048. The authors declare that they have no conflicts of interest with the contents of this article.
[1] Supported by a fellowship from the ANRS.
[2] Present address: Laboratory of Virology and Infectious Diseases, The Rockefeller University, NY 10065.
[3] Present address: CNRS, UMR 5557 Microbial Ecology, Université Lyon 1, Microbial Dynamics and Viral Transmission, 69622 Villeurbanne, France.
[4] Both authors contributed equally to this work.
[5] To whom correspondence may be addressed: CIRI-International Center for Infectiology Research, Team EVIR, Université de Lyon, 69007 Lyon, France. Tel.: 33-472-72-87-32; Fax: 33-472-72-81-37; E-mail: marlene.dreux@ens-lyon.fr.
[6] To whom correspondence may be addressed: CIRI-International Center for Infectiology Research, Team EVIR, Université de Lyon, 69007 Lyon, France. Tel.: 33-472-72-87-32; Fax: 33-472-72-81-37; E-mail: flcosset@ens-lyon.fr.

[7] The abbreviations used are: HCV, hepatitis C virus; HCVcc, cell culture-derived HCV; SR-BI, scavenger receptor BI; LVP, lipoviroparticle; FAH, fumarylacetoacetate hydrolase; NTBC, nitro-4- trifluoromethyl benzoylcyclohexanedione; PHH, primary human hepatocyte; uPA, urokinase-type plasminogen activator; FFU, focus-forming units; HSA, human serum albumin; co-IP, co-immunoprecipitation; hSR-BI, human SRBI; mSR-BI, mouse SR-BI; GE, genome equivalents.

apolipoproteins such as apoB, apoE, and apoC and are then secreted through the Golgi apparatus (1–3).

The association of HCV particles with lipoprotein components such as lipids and apolipoproteins was initially demonstrated for particles retrieved from the peripheral blood of infected patients (4–6). Such HCV particles, called lipoviroparticles (LVPs), resemble very low and low density lipoproteins and have a heterogeneous distribution in densities ranging from less than 1.06 to 1.25 g/ml (7). Cell culture-derived HCV (HCVcc) as well as LVPs can also be immunoprecipitated with antibodies against apoE and apoB (8–10). Moreover, a direct interaction between apoE and viral envelope glycoproteins has recently been demonstrated (11–13), further indicating a close relationship between viral particles and lipoprotein components.

Lipoproteins and their receptors as well as their associated lipid transfer activities are key factors for HCV entry into hepatocytes. Indeed, HCV entry is a multistep process involving the interactions of both viral and cellular components of the LVPs with several host cell receptors. The initial attachment of the virus to the cell is likely mediated by glycosaminoglycans (14), by the LDL receptor (15), and/or by the scavenger receptor BI (SR-BI) (16), which all bind apolipoproteins incorporated on the surface of viral particles. Then, a complex interaction between viral glycoproteins, SR-BI, and other cellular host factors such as the CD81 tetraspanin (17) and the tight junction proteins Claudin-1 (18) and Occludin (19) allows entry and internalization of the viral particles (20). Moreover, other proteins implicated in cholesterol uptake such as Niemann Pick C-1-like 1 (21), and host cell kinases such as the epidermal growth factor receptor and the ephrin receptor A2 (22) have been identified as cofactors of HCV entry. Using the HCVcc and HCV pseudoparticle models, our laboratory recently demonstrated that SR-BI mediates entry of particles independently of their density via its capacity to transfer lipids to and from different carriers (23, 24). Finally, presumably at a further step of entry, HCVcc particles of lower-intermediate density (*i.e.* 1.08–1.13 g/ml) and HCV pseudoparticles become able to bind SR-BI via a direct interaction with the E2 glycoprotein, which results in enhancement of their entry process (23–25).

HCV assembly and release have mainly been studied using the highly infectious molecular clone JFH1 or using JFH1-derived recombinant viruses produced in hepatoma cell lines (26–29). However, most of these cell lines have impaired production of VLDL because they express pre-VLDLs that are not fully lipidated and that do not fuse with apoE-containing luminal lipid droplets (30). The resulting HCVcc particles are thus poorly associated with apoB (9), and their buoyant density profile is significantly different compared with *in vivo* recovered viruses (31, 32). As lipid and apolipoprotein components are key factors influencing HCV biology, this highlights the need to better understand how they are distributed within the different forms of HCV particles circulating *in vivo* and how such distributions functionally influence their entry properties. Importantly, HCV particles from infected patients are not or not robustly infectious *ex vivo*, thus precluding their functional characterization.

A major advance in the study of HCV infection *in vivo* was made due to the development of immunodeficient mice that sustain human hepatocyte engraftment (33, 34). Using the AlbuPA/SCID mouse model, Lindenbach *et al.* (31) showed that HCV physical particles, as assessed by viral RNA distribution, have a lower density compared with HCVcc particles; however, the infectivity of such viral populations remained undermined. Although this study suggested that viruses issued from infected mice may have a higher specific infectivity compared with *in vitro* cultured virus (31), to our knowledge, there is no study describing the composition (in terms of viral and cellular components) of HCV particles issued from these mice as well as their entry properties.

Here, we characterize HCV particles and viral subpopulations produced in humanized liver mice derived from the FRG mouse model (further designated HCVfrg), a triple mutant mouse knocked out for fumarylacetoacetate hydrolase (FAH), RAG2, and γ_c (35) that was previously shown to support HCV infection (36). We demonstrate that, unlike HCVcc, the most infectious *in vivo* recovered HCVfrg particles are highly enriched in apoE. Moreover, our work features further differences between HCVfrg and HCVcc because we show that HCVfrg particles exhibit a strongly increased dependence on SR-BI expression levels for entry of HCVfrg particles of very low density. Finally, we show that entry of HCVfrg particles of all densities is strongly dependent on the lipid transfer activity of SR-BI rather than on its binding to the viral glycoprotein E2. Thus, altogether, our results suggest that the lipoprotein components incorporated on viral particles play a crucial role in entry of infectious particles, and our results highlight the powerfulness of this *in vivo* model for the functional study of the interplay between HCV and liver components.

Experimental Procedures

Cell Lines—Huh-7.5 and 293T cells were grown in DMEM (Invitrogen) supplemented with 100 units/ml penicillin, 100 μg/ml streptomycin, and 10% fetal bovine serum.

Mouse Colony Maintenance, Nitro-4-trifluoromethyl Benzoylcyclohexanedione (NTBC) Cycling, and Primary Human Hepatocyte (PHH) Engraftment—FRG (*Fah*$^{-/-}$*Rag2*$^{-/-}$*Il2rg*$^{-/-}$) mice (mixed background: C57BL/6 and 129Sv) were provided by M. Grompe (Oregon Health and Science University) and bred in our animal facility (Plateau de Biologie Expérimentale de la Souris, Lyon, France).

FRG mice are deficient for the FAH enzyme, which leads to an accumulation of a toxic tyrosine catabolite in the liver. To prevent this toxicity, mice are maintained on 8 mg/liter NTBC (Swedish Orphan Biovitrum) in the drinking water. NTBC acts by blocking the tyrosine catabolic pathway upstream of FAH and thus prevents the accumulation of toxic metabolites. FRG mice were kept in temperature- and humidity-controlled animal quarters with a 12-h light/12-h dark cycle.

PHHs were injected intrasplenically as described previously (34). Immediately after engraftment, the NTBC was progressively withdrawn as follow: 2 days at 10% of colony maintenance concentration, then 2 days at 5%, and 2 days at 2.5%, and then the NTBC was completely removed. During the phase without NTBC, mice were weighed every 2 days. After 2–6 weeks, mice

with clinical symptoms (lethargy and hunched posture) or severe weight loss (>15%) were again put on NTBC for 3 days before a second withdrawal (cycling). Cycling was repeated until clinical symptoms resolved. To prevent the development of a murine hepatocellular carcinoma, highly reconstituted mice selected for infectious experiments were subjected to further NTBC treatment (3–4 weeks without NTBC and 3 days with 100% NTBC). No other drugs were administered during the entire study. 48 h prior to engraftment, adult (6–10 weeks old) mice were injected intravenously with 2×10^9 pfu of an adenoviral vector encoding the uPA transgene. 7×10^5–1×10^6 PHHs (BD Biosciences) were injected intrasplenically, and NTBC was progressively withdrawn. Experiments were performed in accordance with the European Union guidelines for approval of the protocols by the local ethics committee (Authorization Agreement C2EA-15, *Comité Rhône-Alpes d'Ethique pour l'Expérimentation Animale*, Lyon, France).

Immunohistochemistry Antibodies and Methods—For histological examination, liver tissues from FRG mice were fixed in 10% buffered formalin and embedded in paraffin. 4-μm-thick sections were prepared according to conventional procedures, stained with hematoxylin-phloxine-saffron, and observed with a light microscope. Immunohistochemistry was performed using a panel of primary antibodies against FAH (Aviva Systems Biology, San Diego, CA), *carcinoembryonic antigen* (Novus Biologicals, Littleton, CO), CD31, CD34, CK7, and CK18 (all from Dako, Glostrup, Denmark). These antibodies only reacted with human tissue.

An automated immunostainer (Ventana Discovery XT, Roche Applied Science) was used with the DABmap kit according to the manufacturer's instructions. A standard horseradish peroxidase staining procedure was followed. All sections were counterstained with Gill's hematoxylin. As negative controls, slides were stained without the primary antibody. Slides were analyzed in a Mirax slide scan (Zeiss, Jena, Germany).

The repopulation index was determined by using an ImageJ macro program. Images were split into their color components based on *3,3′-diaminobenzidine* staining (color deconvolution), then automatically thresholded, and measured. Results were collected in a comma-separated value table. The repopulation index was calculated based on the surface ratio between the *3,3′-diaminobenzidine*-positive surface and the total surface.

Serological and Immunohistochemical Analyses—Blood from transplanted mice and controls was collected every 2–4 weeks after engraftment by retro-orbital puncture. Sera were sent to a diagnostic laboratory for quantification of human serum albumin (Cobas C501 analyzer, Roche Applied Science). For lipoprotein analyses, sera were run on a Lipoprint Lipoprotein Subfractions Testing System (Quantimetrix) that quantifies lipoprotein fractions (VLDL, LDL, and HDL) on the basis of their cholesterol amount. Human apoB and apoE concentrations were measured in FRG mouse sera and human samples by ELISA (Mabtech, Sweden) according to the manufacturer's instructions.

HCVcc Production—In vitro transcribed RNA was electroporated into Huh-7.5 cells. 72 h postelectroporation, infectious titers were determined as focus-forming units (FFU)/ml estimated by NS5A immunostaining and colony counting as described previously (37). Infectious titers were between 1 and 2×10^5 FFU/ml.

Virus Inoculation and Blood Analysis—Highly reconstituted mice (human serum albumin (HSA) >15 mg/ml) were infected with 1×10^5 FFU of HCV of genotype 2a of the Jc1 chimera (29) by the intraperitoneal route. 100 μl of total blood were collected every week, and HCV RNA and viral infectivity were measured. RNA was extracted with a guanidine thiocyanate method, reverse transcribed (iScript cDNA synthesis kit, Bio-Rad), and quantified with the FastStart Universal SYBR Green Master kit (Roche Applied Science) on an Applied StepOne Real-Time PCR apparatus using HCV-specific primers (5′-TCTGCGGAACCGGTGAGTA and 5′-TCAGGCAGTACCACAAGGC). As an internal control of extraction, an exogenous RNA from the linearized Triplescript plasmid pTRI-Xef (Invitrogen) was added into the sera prior to extraction and quantified with specific primers (5′-CGACGTTGTCACCGGGCACG and 5′-ACCAGGCATGGTGGTTACCTTTGC).

Iodixanol Gradient Separation of HCV Particles—800 μl of serum from infected mice or HCVcc virus-containing supernatants were loaded on top of a 3–40% continuous iodixanol gradient (Optiprep, Axis Shield). Gradients were centrifuged for 16 h at 4 °C in an Optima L-90 centrifuge (Beckman).

Co-Immunoprecipitation (Co-IP) of Apolipoproteins and Viral RNA—Co-IPs of apolipoprotein-HCV RNA from HCVfrg and HCVcc were performed on 100 μl of non-fractionated samples or on iodixanol-separated fractions. Samples were run in a 3–40% iodixanol gradient. Seven fractions of 1500 μl were collected from the top of the gradient, and 1100 μl were used for co-IP experiments. Samples were precleared with 40 μl of protein G magnetic beads (Millipore) for 1 h at 4 °C. For preabsorption of antibodies to protein G magnetic beads, 6 μl of polyclonal goat anti-apoE (AB947, Millipore) or anti-apoB (AB742, Millipore) or goat immunoglobulins (IP control) were mixed with 40 μl of beads in a total volume of 100 μl and incubated 1 h at 4 °C. The precleared samples were added to the antibody-coated beads and incubated for 3 h at 4 °C under continuous rotation. The immune complexes were washed three times in PBS, and beads were resuspended in guanidine thiocyanate buffer for HCV RNA extraction and quantification or alternatively in lysis buffer for Western blot analysis.

Establishment of Cell Lines Expressing WT or Mutant SR-BI—Retroviral vectors expressing human SRBI (hSR-BI), mouse SR-BI (mSR-BI), or the hSR-BI point mutant G420H/G424H were generated and expressed in Huh-7.5 cells as described previously (24). Down-regulation of hSR-BI was achieved using two small interfering RNAs (5′-GCAGCAGGUCCUUAAGAAC and 5′-GGCACTGTTCTGGAACCTTC) as described previously (38). SR-BI overexpression was verified by FACS analysis (CLA-1 antibody, BD Pharmingen) or by Western blot analysis (NB400-104 antibody, Novus).

Neutralization Assays—Huh-7.5 cells overexpressing hSR-BI were preincubated with the anti-SR-BI antibody NK-8H5-E3 (39) or with control IgGs for 1 h at 37 °C at a final concentration of 10 or 100 μg/ml. Cells were then infected with dilutions of non-fractionated viruses or with gradient density-separated fractions of HCVfrg and HCVcc particles. Infectivity was measured 72 h postinfection by immunostaining the viral glycopro-

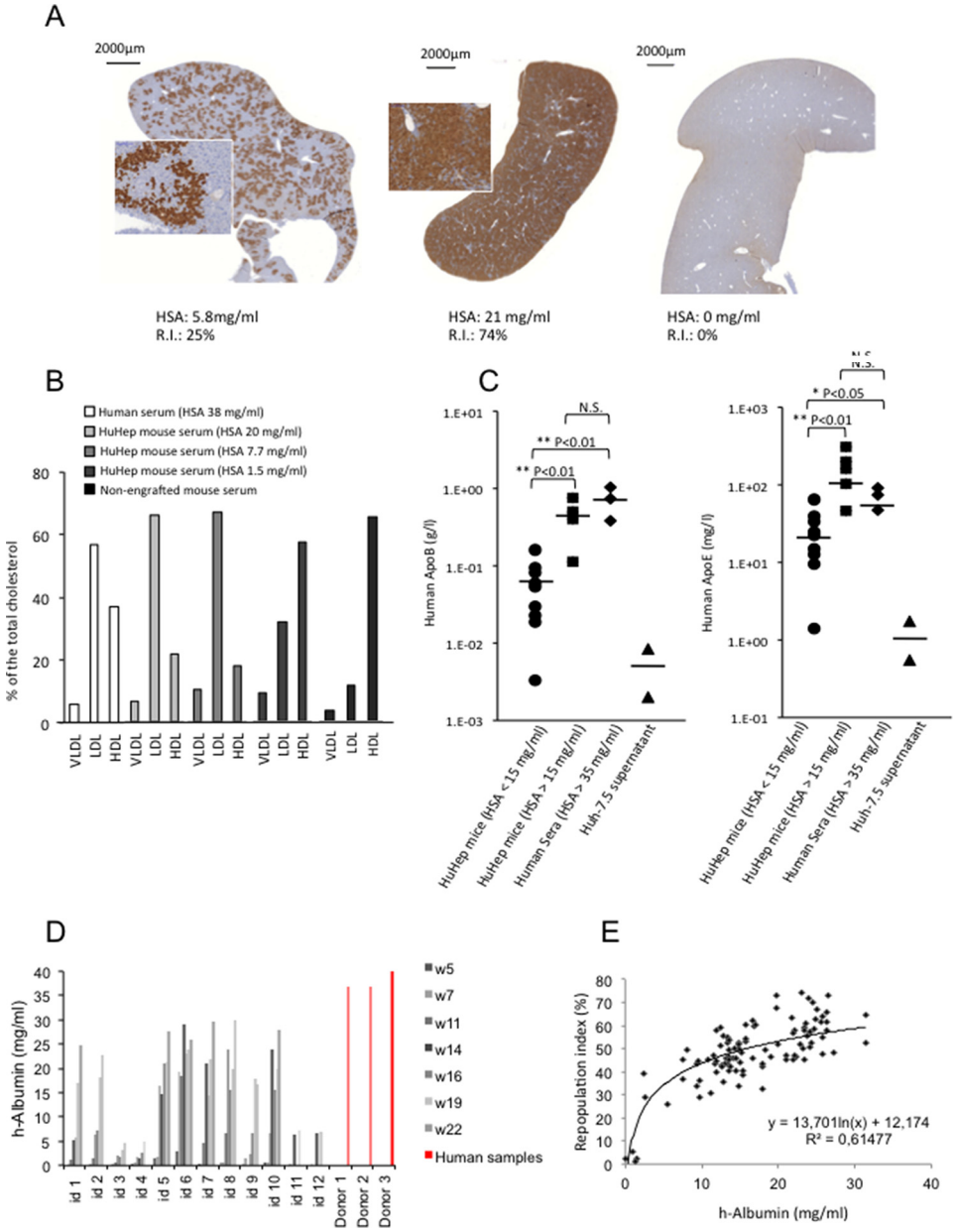

FIGURE 1. **Highly repopulated liver chimeric mice sustain HCV infection.** *A*, human FAH staining of a moderately liver-reconstituted mouse, a highly liver-reconstituted mouse, and non-engrafted mouse. *R.I.*, repopulation index. *Original magnifications*, ×15 and ×400 (*insets*). *B*, lipoprotein distribution in the sera from FRG mice reconstituted at different levels as indicated by HSA levels in mg/ml and human sera or non-engrafted FRG mouse sera as control. Sera were run on a Lipoprint system, and cholesterol content was measured within each lipoprotein fraction. Results represent the percentage of cholesterol in each subpopulation compared with total cholesterol. *C*, quantification of human apoB and apoE in the serum of human liver-reconstituted mice, human individuals, and supernatant from confluent Huh-7.5 cells. Statistical analyses were performed by a Mann-Whitney test. *N.S.*, not statistically significant. *D*, follow up of HSA in human liver engrafted FRG mice (*id 1–12*). As a comparison, HSA was measured in plasma or sera from three healthy individuals (*Donors 1–3*). To note, HSA levels in engrafted mice are in accordance with a recently published study on humanized liver in NOD FRG mice (65). *E*, correlation between HSA and the repopulation index that represents the percentage of human FAH-positive cells in liver sections from PHH-engrafted FRG mice. *h*, human; *w*, week; *HuHep*, human hepatocytes.

tein E2 using the human recombinant AR3A antibody (Ref. 40; a kind gift from M. Law).

Results

FRG Mice with Highly Reconstituted Human Liver Allow Productive HCV Infections—We first sought to validate that, in our experimental conditions, engraftment of FRG mice with primary human hepatocytes allows a robust liver reconstitution and thus a sustained HCV infection as described previously (36). 11–16 weeks postengraftment, HSA levels were higher than 15 mg/ml (range, 16–29 mg/ml) in 65% of the engrafted mice, *i.e.* close to the human physiologic concentrations (Fig. 1*D*). Human FAH immunostaining in liver sections confirmed a high and homogeneous repopulation with PHHs (Fig. 1*A*) with a good correlation between HSA values and the extent of human liver reconstitution (Fig. 1*E*). Overall, in 76% of the mice, liver repopulation with PHHs was higher than 40%. Next, we investigated whether highly human liver-reconstituted mice were able to secrete human lipoproteins. Mice rely on HDL for their cholesterol supply, whereas in humans, LDL and VLDL

are the preponderant cholesterol-supplying lipoproteins. Accordingly, the determination of the LDL *versus* HDL proportion revealed that although sera from mice with low levels of human liver reconstitution are enriched with high density lipoproteins the profiles of highly human liver-reconstituted mice, as assessed by HSA levels, approached the human profiles, *i.e.* characterized by a preponderance of low density lipoproteins (Fig. 1*B*). Finally, highly liver-reconstituted FRG mice (HSA >15 mg/ml) secreted high levels of human lipoproteins close to human physiological concentrations (Fig. 1*C*). The histological analyses of human liver-reconstituted mice further confirmed that highly repopulated chimeric livers had a normal and functional liver architecture in which human hepatocytes of different degrees of maturation as well as a human bile canalicular network and sinusoid vessels were observed (Fig. 2).

Engrafted mice with HSA levels over 15 mg/ml were infected with 10^5 FFU of HCVcc of genotype 2a (Jc1 chimera). The amount of HCV RNA detected in the sera increased steadily over time after infection to reach a plateau level at approximately 7 days postinoculation as described previously (36), and HCV infection was robust and sustained in all of the inoculated mice with both viral RNA (range, 10^5–10^8 genome equivalents (GE)/ml) and infectious particles (range, 10^3–10^6 FFU/ml) being detected for at least 4 weeks (Fig. 3*A*). Importantly, HCVfrg viral loads were comparable with HCV RNA titers measured in infected individuals in acute phase (range, 5×10^4–5×10^8 GE/ml) (41).

HCVfrg Infectious Particles Have a Lower Density as Compared with HCVcc—Four weeks after infection, animals were sacrificed, and total blood was collected. Infected sera were loaded on continuous density gradients and separated in 15 fractions. Viral RNA and infectious virus levels were determined for each fraction. Buoyant density analysis revealed the distribution of HCVfrg RNA within two major RNA populations (Fig. 3*B*), the first in the 1.06–1.11 g/ml density range and the second in the 1.11–1.16 g/ml density range. Interestingly, the viral RNA population of lower density overlapped with the infectious population (Fig. 3*B*), showing that most of the infectious virus (~90%; range, 80–100%) had a density between 1.06 and 1.11 g/ml, whereas a large amount of physical particles, *i.e.* those of higher density, was not or very poorly infectious.

As a comparison, similar fractionation experiments were performed using HCVcc, and they raised important differences compared with HCVfrg particles. Indeed, we found that the buoyant density of the HCVcc infectious viral population was more heterogeneous as compared with HCVfrg (Fig. 3*C*). Indeed, 90% of HCVcc infectious particles were distributed among density fractions of 1.03–1.13 g/ml in contrast to the more restricted range of density of infectious HCVfrg (*i.e.* 90% in density fractions of 1.06–1.11 g/ml). Furthermore, the highest infectivity of HCVcc infectious particles was shifted among higher density fractions (1.08–1.13 g/ml) with a peak around 1.10 g/ml (Fig. 3*C*), whereas most physical particles were detected within fractions of 1.10–1.15 g/ml with a peak around 1.12 g/ml (Fig. 3*C*). Interestingly, viruses recovered *in vivo* had a approximately 100-fold augmentation in their specific infectivity (HCVfrg, 5.3×10^{-2} FFU/GE; HCVcc, 4.2×10^{-4} FFU/GE) as calculated by the median of the specific infectivity of each HCVfrg and HCVcc sample (Fig. 3, *B* and *C*, *insets*). Altogether, these results indicated that *in vivo* produced infectious HCVfrg particles are highly infectious and have a lower and more homogenous density as compared with cell culture-derived virus. These differences of biophysical properties imply that HCVfrg and HCVcc likely differ in terms of lipid and/or protein composition.

Highly Infectious HCVfrg Populations Are Enriched with ApoE—Therefore, we sought to determine whether the difference in density profiles between HCVfrg and HCVcc infectious particles was due to a differential association of the virus with lipoprotein components. To separate viral particles from lipoproteins, we performed co-IP assays using antibodies against apolipoproteins apoE and apoB, and we quantified the captured particles by HCV RNA-specific RT-quantitative PCR. We decided to use this approach because previous papers showed that the initial capture of viral particles with anti-E2 antibodies was inefficient probably because of poor epitope accessibility (9, 10). We first performed co-IP assays on non-fractionated samples using apoE or apoB antibodies. We could immunoprecipitate 57% (mean ± 29%; $n = 7$) and 30% (mean ± 20%; $n = 9$) of HCVcc viral RNA using anti-apoE- and anti-apoB-coated beads, respectively. In contrast, we could co-immunoprecipitate 23% of total HCV RNA of HCVfrg particles with apoE antibodies (mean ± 20%; $n = 10$) but less than 5% with apoB (mean ± 5%; $n = 8$) antibodies (data not shown). The weak apoB capture of HCV particles from HCV-infected human liver-reconstituted FRG mouse samples is likely to depend on the high concentration of apoB in the sera of human liver-reconstituted FRG mice (Fig. 1*C*), which may compete with apoB present on viral particles for the binding to the antibody. Indeed, addition of serum from non-infected human liver-reconstituted FRG mice to HCVcc particles decreased the co-IP rates by about 10-fold (data not shown). Moreover, the dissimilarities in co-IPs results of HCVfrg *versus* HCVcc particles could be due to a different lipidation of either type of viral particle and thus to a differential exposure of apoE and apoB proteins on their surface.

We then performed co-IPs of apoE-HCV RNA on density gradient-separated viral subpopulations. First, we sought to assess the distribution of apoE along the different buoyant density-separated fractions. Although the distribution of apoE in HCVcc samples was homogeneous among the different subpopulations (Fig. 4*B*), apoE was predominantly present in low density fractions of HCVfrg samples (*i.e.* <1.06 g/ml) (Fig. 4*A*). Nevertheless, apoE could be readily immunoprecipitated all along the gradient for both HCVcc and HCVfrg samples (Fig. 4, *A* and *B*).

To verify that this difference was due to a different lipid composition of mouse sera *versus* cell culture supernatants and not to viral components, uninfected mouse sera were subjected to gradient density separation, and apoE distribution was analyzed by Western blot analysis. The results showed a similar distribution of apoE among fraction samples derived from HCV-infected or uninfected mouse sera (Fig. 4, *A* and *C*), thus confirming a different composition of lipoproteins between the HCVfrg and HCVcc models.

Interestingly, when comparing apoE-HCV RNA co-immunoprecipitation in HCVfrg *versus* HCVcc samples sepa-

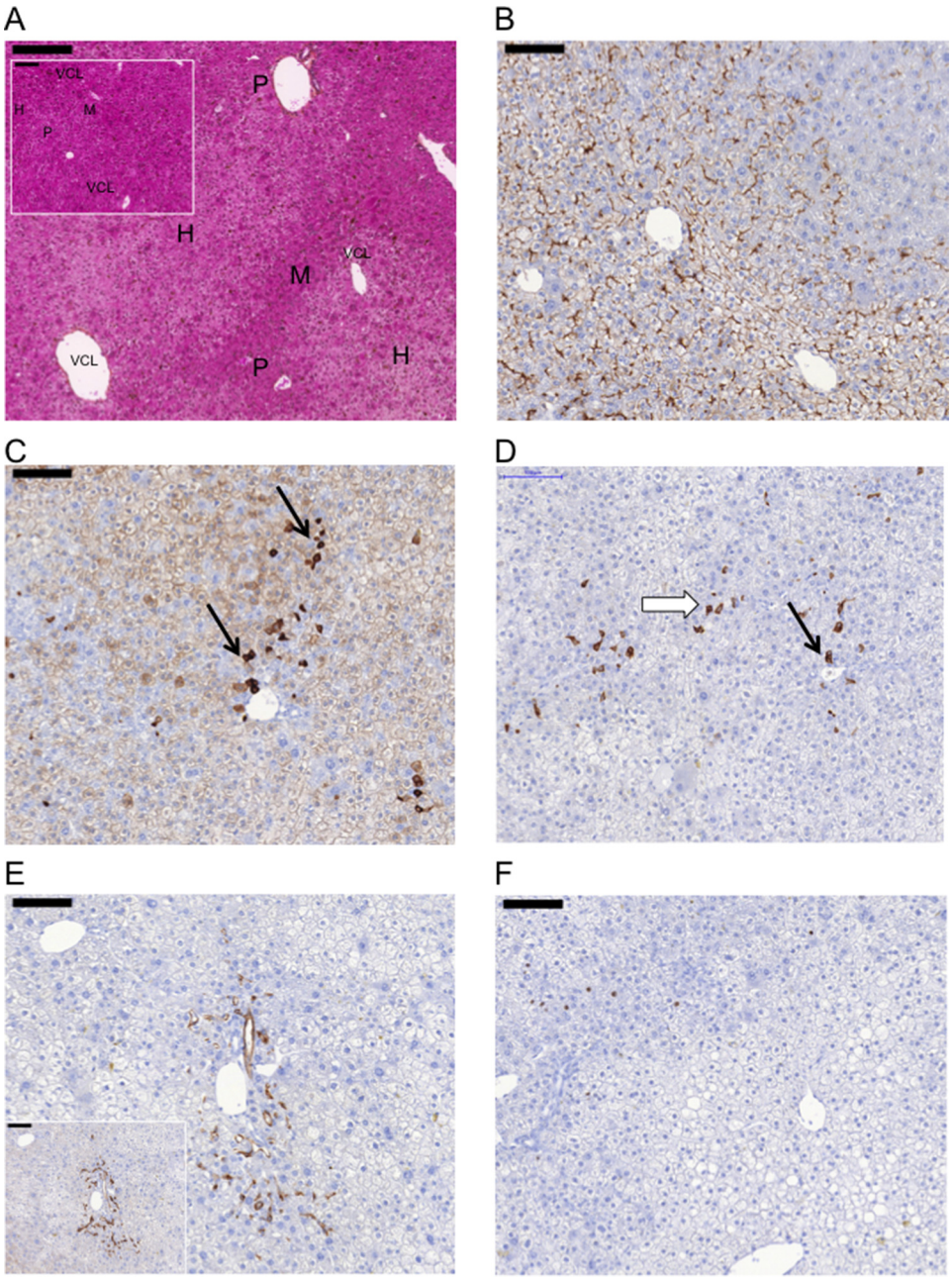

FIGURE 2. **Highly repopulated chimeric livers maintain a normal and functional liver architecture.** *A*, hematoxylin-phloxine-saffron staining reveals that liver parenchyma is repopulated by pale human hepatocytes. Human hepatocyte aggregates are easily discerned after hematoxylin-eosin staining because of their large size, abundant cytoplasm, and large nuclei containing dispersed chromatin with well formed nucleoli. *B*, immunodetection of human-specific *carcinoembryonic antigen* confirms the capacity for human hepatocytes to form bile canaliculi; the bile canalicular network is as dense and organized as in normal human liver. *C*, human hepatocytes are also detected with anti-human CK18. Mature human hepatocytes present a pale staining, whereas human hepatic progenitor cells are strongly immunoreactive for CK18. The *black arrow* indicates human hepatic progenitors. *D*, staining with anti-human CK7 confirms the presence of immature hepatocytes (*white arrow*), which are surrounded by mature hepatocytes that do not stain for CK7. After immunodetection of CK18 and CK7 (*C* and *D*), it is possible to identify human bile ducts cells (CK7+) and CK7+/CK18+ small to intermediate sized cells with moderately abundant cytoplasm and excentered nuclei; they are similar to the so-called intermediate cells observed during human liver regeneration after injury or cell loss. Anti-human CK7 also stains human bile ducts cells (*black arrow*). *E*, within human hepatocyte aggregates, cells are arranged in plates of variable thickness separated by well formed sinusoid vessels lined by CD31+ or CD34+ (*inset*) endothelial cells. *F*, the presence of a few Ki67-positive cells, preferentially at the junction between human and murine hepatocytes, indicates proliferation of human hepatocytes in close proximity to dying murine hepatocytes. *Original magnifications*, ×400 (×200 for *A* and ×400 for *inset*). *Scale bar*, 100 μm (200 μm for *A* and 100 μm for *inset*). *H*, human hepatocytes; *M*, murine hepatocytes; *VCL*, centrolobular vein; *P*, portal track.

rated on density gradients, we found that although for HCVcc particles (Fig. 4*E*) apoE-enriched particles were distributed throughout the gradient without marked overlap with infectious populations the distribution of apoE-co-immunoprecipitated HCVfrg particles coincided with the highly infectious population (*i.e.* at a density range of 1.06–1.11 g/ml) (Fig. 4*D*). To rule out that the quantity of antibody was limiting for the immunoprecipitation of highly apoE-enriched fractions, we performed co-IP assays with a 10 times greater quantity of antibody than we otherwise used

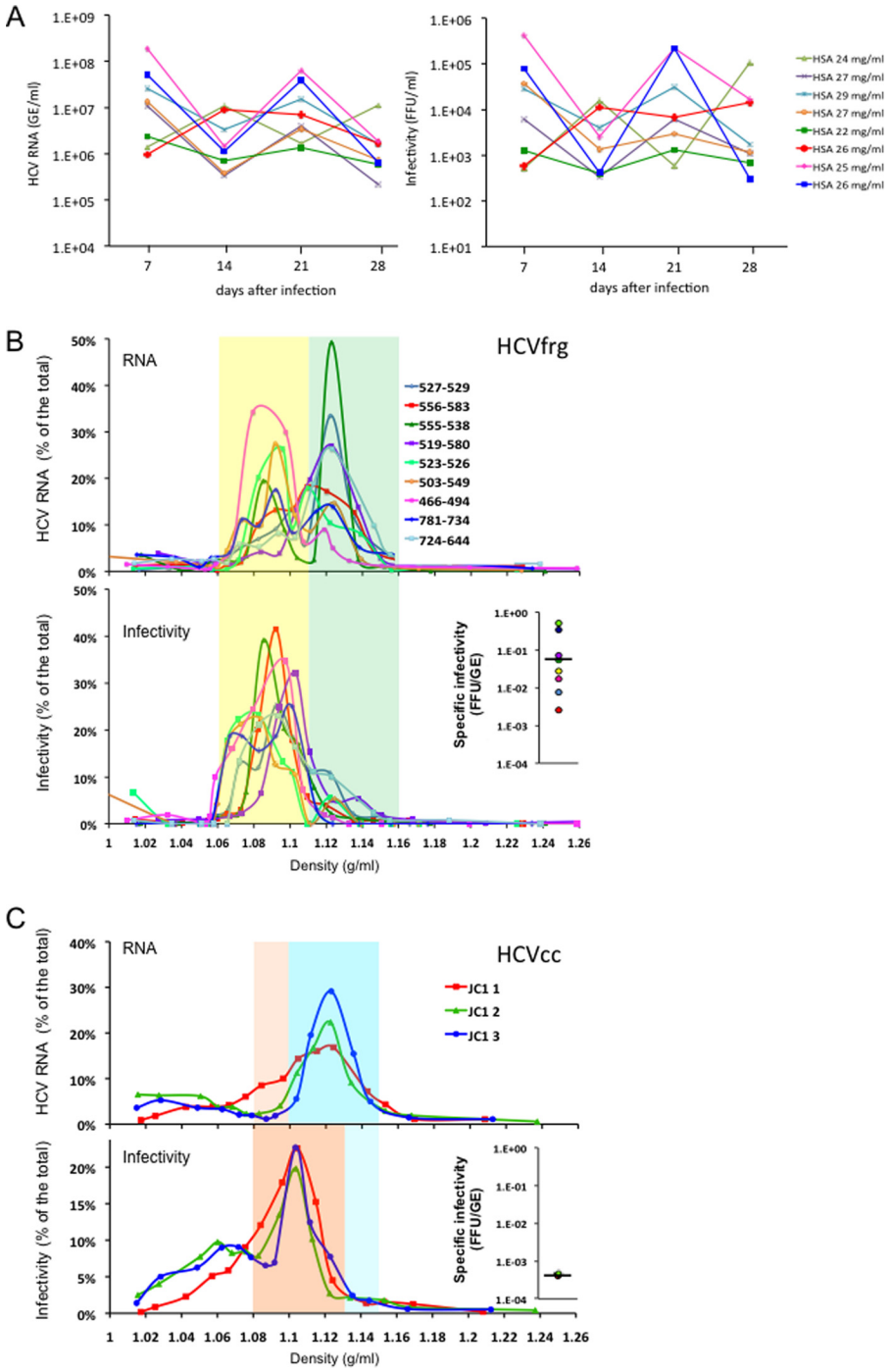

FIGURE 3. **Highly infectious HCVfrg populations have a lower density compared with HCVcc viral particles.** *A*, time course quantification of HCV RNAs and infectious virus levels in mice sera after inoculation with 10^5 FFU of Jc1 virus (HCV2a genotype). HSA levels at the time of the inoculation are reported in the chart legend. HCV RNA and infectious viruses were not detected at any time points in the controls (*i.e.* engrafted mice with mock inoculation and non-engrafted mice inoculated with HCV; data not shown). The detection limits of the quantification of HCV RNA and infectivity are 2×10^4 GE/ml and 5×10^2 FFU/ml, respectively. *B*, sera from humanized liver FRG mice. Because of the limited volume of serum available from each mouse, they were pooled two by two to obtain a high resolution gradient with several fractions. *Numbers* indicate mice identification numbers. *C*, supernatants from HCVcc-infected Huh-7.5 cells. Three independent experiments were performed (*JC1 1–3*). Samples were run overnight in a 3–40% iodixanol gradient. Fifteen fractions were collected, and HCV RNA and infectivity were measured. Results are reported as the percentage of RNA or infectivity in each fraction relative to the total. In HCVfrg (*B*), RNA (*top graph*) is distributed in two main populations with a density of 1.06–1.11 and 1.11–1.16 g/ml (defined by *yellow* and *green boxes*, respectively), whereas infectivity (*bottom graph*) is uniformly distributed within one population (*yellow box*) of 1.06–1.11 g/ml. In HCVcc (*C*), RNA (*top graph*) is mainly distributed around the fractions with a density of 1.10–1.15 g/ml (*blue box*), whereas infectivity (*bottom graph*) is mostly detected in fractions of 1.08–1.13 g/ml (*orange box*). *Insets*, specific infectivity expressed as the number of infectious particles/physical particles (ratio FFU/GE). The *horizontal bars* represent the median values. HCVfrg, $n = 9$; HCVcc, $n = 3$.

for such experiments (as in Fig. 4*D*), and we found that the distribution of the co-immunoprecipitated apoE-HCV RNA complexes had the same profile regardless of the apoE antibody concentration (data not shown).

Thus, in sharp contrast with HCVcc, apoE was reproducibly enriched in specific HCVfrg populations representing the most infectious particles. This reflected the homogeneity of HCVfrg infectious particles. In accordance with the *in vitro* studies of

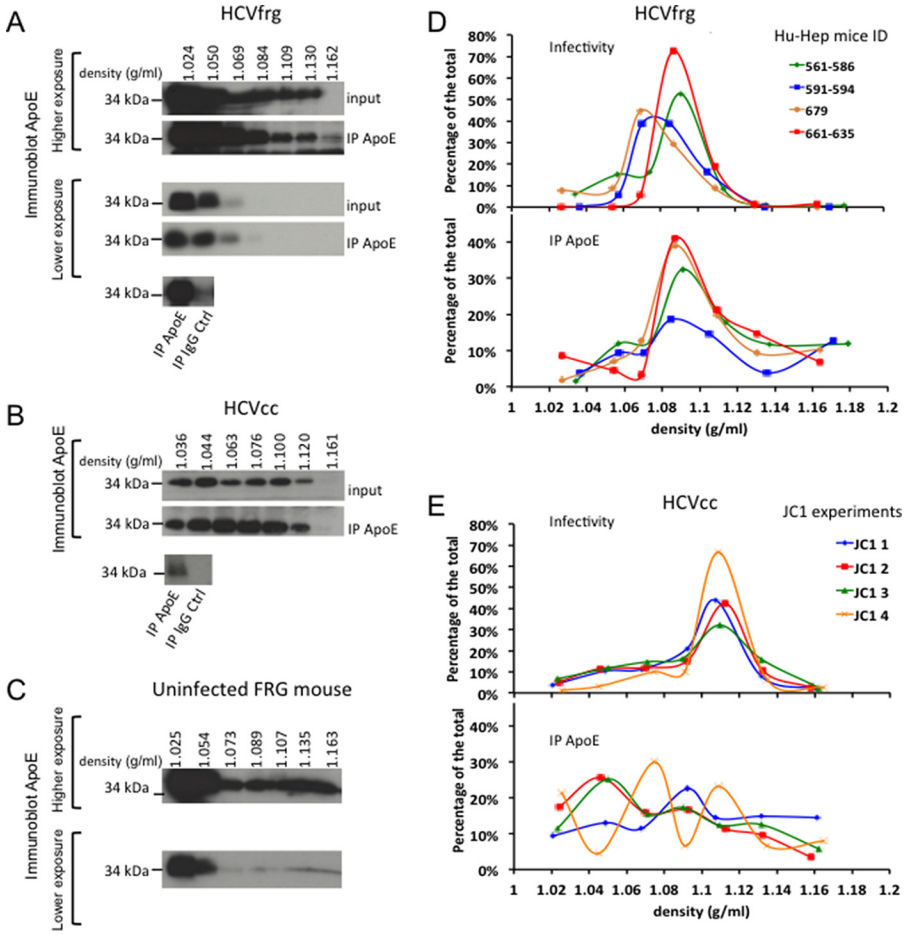

FIGURE 4. **Highly infectious HCVfrg particles are enriched in apoE.** The distributions of apoE in buoyant density-separated fractions of HCVfrg (*A*), HCVcc (*B*) samples, and serum of an uninfected FRG mouse (*C*) are shown. 50 μl of each fraction as well as their respective apoE-immunoprecipitated complexes were lysed in a denaturing buffer and stained with a polyclonal goat anti-apoE antibody (AB947). In *A* and *C*, the *upper panel* corresponds to a high film exposure, whereas the *lower panel* corresponds to a low exposure. As a control for unspecific binding, non-fractionated HCVfrg and HCVcc samples were subjected to immunoprecipitation with goat IgG-coated magnetic beads (IgG Ctrl). The distributions of infectivity and of co-immunoprecipitated complexes of apoE-HCV RNA in buoyant density-separated HCVfrg (*D*) and HCVcc (*E*) are shown. ApoE IP values are calculated as a percentage of co-immunoprecipitated RNA relative to the total RNA within each fraction using an equivalent volume for each fraction. *JC1 1–4* are from four independent experiments.

apoE function, our findings suggested that apoE is an essential factor for entry of infectious *in vivo* produced virus (23, 42–46).

HCVfrg Show an Uneven Dependence on SR-BI for Entry of Viral Subpopulations—Previous results from our laboratory indicated that specific functions of SR-BI are implicated in entry of HCVcc subpopulations in a manner dependent on the physicochemical properties of the viral particles (23). Importantly, the comparison of HCVfrg and HCVcc particles highlighted substantial dissimilarities in the apoE content of the different viral particle subpopulations (Fig. 4). Because apoE incorporated on virions acts as a ligand of SR-BI for HCV entry into cells (23, 42), we first sought to investigate the reliance on SR-BI for entry of HCVfrg subpopulations.

Thus, we modulated expression of human SR-BI in Huh-7.5 cells (Fig. 5*A*) to determine infectious titers and SR-BI dependence of HCVfrg subpopulations. We found that infectivity of non-fractionated HCVfrg as well as of HCVcc (Fig. 5, *B* and *C*) particles was decreased and increased by about 10 times in SR-BI down- and up-regulated cells, respectively. This indicated that, similarly to HCVcc, HCVfrg particles rely on SR-BI for entry into cells.

Consistently, in fractionated HCVfrg and HCVcc samples, SR-BI down-regulation resulted in a pronounced and uniform diminution of infectivity (Fig. 5, *D* and *E*) regardless of their density, thus confirming the importance of this receptor for entry. Moreover, SR-BI overexpression stimulated entry of both HCVfrg and HCVcc subpopulations (Fig. 5, *D–F*), particularly those that exhibited the highest infectivity (*i.e.* in fractions 1.06–1.11 and 1.08–1.13 g/ml, respectively). Interestingly, in sharp contrast to HCVcc, gradient density-separated HCVfrg viral subpopulations showed an uneven dependence on SR-BI for entry. Indeed, the effect of SR-BI overexpression on HCVfrg infectivity was specifically marked in the very low density fractions (Fig. 5*F*). This was particularly salient for HCVfrg particles of density $<$1.05 g/ml for which at least 10–100-fold higher infectious titers could be detected (Fig. 5, *D* and *F*). This indicated that SR-BI expression is limiting for entry of low density HCVfrg particles, which highlighted a further difference between HCVfrg and HCVcc.

To confirm SR-BI dependence for entry of HCVfrg viral subpopulations, cells were incubated prior to infection with the SR-BI antibody NK-8H5-E3 that has been shown previously to block

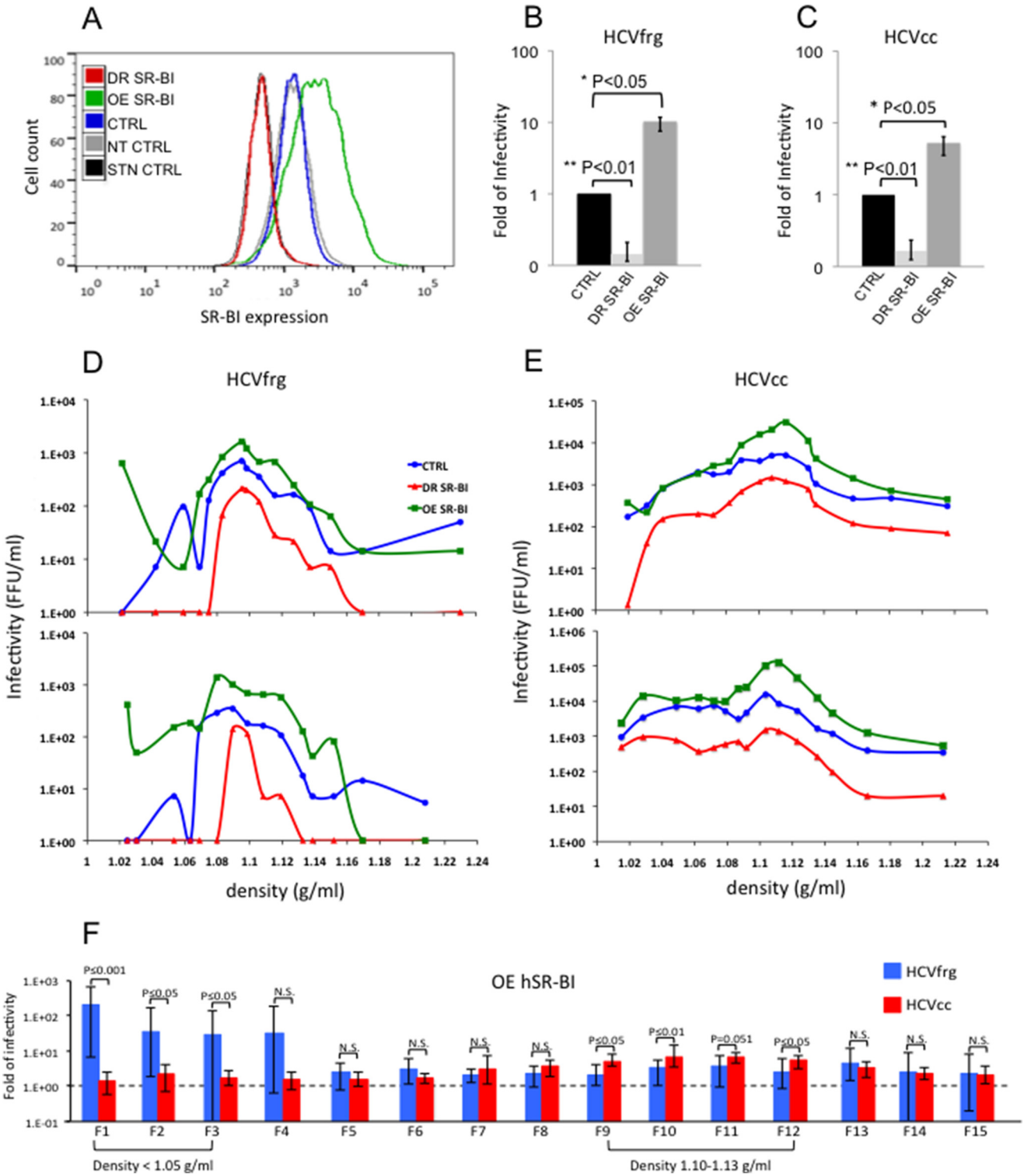

FIGURE 5. **SR-BI expression differentially modulates entry of HCVfrg and HCVcc viral subpopulations.** *A*, flow cytometry analysis of Huh-7.5 cells over-expressing (*OE*) or down-regulating (*DR*) SR-BI at the time of HCV infection. Huh-7.5 cells were transduced with two bicistronic lentiviral vectors coding small interfering RNAs (SR-BI/siRNA-2 and SR-BI/siRNA-24) together with the GFP protein (*DR SR-BI*, down-regulation of SR-BI) or with a lentiviral vector coding human SR-BI (*OE SR-BI*, overexpression of SR-BI). *CTRL*, cells transduced with the backbone vector expressing the GFP; *NT CTRL*, non-transduced cells; *STN CTRL*, staining without the primary antibody. Transduced cells were infected with serial dilutions of sera from non-fractionated HCVcc-infected mice (*B*) or of supernatants from HCVcc-infected Huh-7.5 cells (*C*). As a control, cells were transduced with the backbone vector expressing the GFP. Infection levels were within a range of 1.3×10^4–3.9×10^4 FFU/ml and 2.2×10^4–5.3×10^4 FFU/ml for HCVfrg and HCVcc, respectively. Statistical analysis was performed by Student's *t* test ($n = 3$). SR-BI down- or up-regulated cells were infected with HCVfrg (*D*) or HCVcc (*E*) using serial dilutions of gradient density-separated fractions. Examples of distribution of infectivity from two humanized liver FRG mice (*D*) and from two HCVcc independent experiments (*E*) are shown. *F*, -fold increase of infectivity of HCVfrg and HCVcc subpopulations in hSR-BI-overexpressing cells compared with the controls. Results are the average of seven HCVfrg and six HCVcc independent experiments and are shown for each density fraction (*F1–F15*). Statistical analyses were performed by a Mann-Whitney test. *N.S.*, not statistically significant. *Error bars* represent S.D.

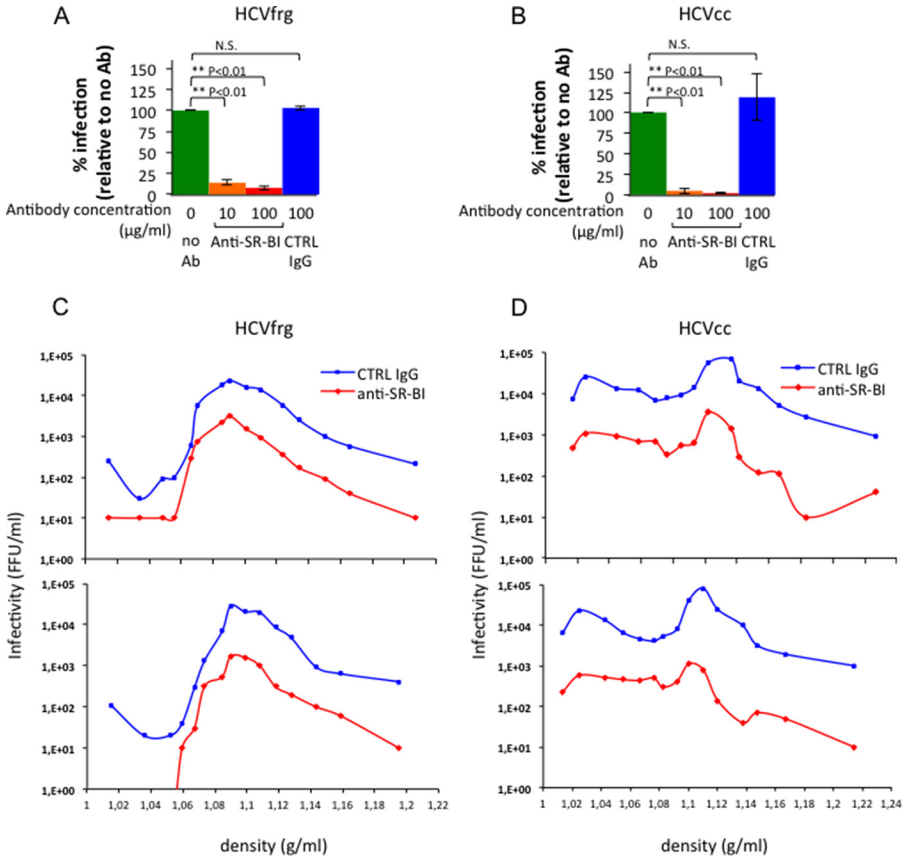

FIGURE 6. **SR-BI antibody blocks entry of HCVfrg and HCVcc viral subpopulations.** Cells overexpressing hSR-BI (Fig. 5*A*) were preincubated with the indicated concentrations of the NK-8H5-E3 SR-BI-blocking antibody (*Anti-SR-BI*) or a control isotype (*CTRL IgG*). Cells were subsequently infected with serial dilutions of non-fractionated sera from HCVcc-infected mice (*A*) or non-fractionated supernatants from HCVcc-infected Huh-7.5 cells (*B*). Infection levels in the absence of antibody were within a range of 3.4×10^3–1.5×10^4 and 6.7×10^4–1.8×10^5 FFU/ml for HCVfrg and HCVcc, respectively. Statistical analysis was performed by Student's *t* test ($n = 3$). *N.S.*, not statistically significant. *Error bars* represent S.D. SR-BI-up-regulated cells were preincubated with the NK-8H5-E3 antibody (*Anti-SR-BI*) or a control isotype (*CTRL IgG*). Cells were then infected with HCVfrg (*C*) or HCVcc (*D*) using serial dilutions of gradient density-separated fractions. Representative distributions of infectivity from two humanized liver FRG mice (*C*) and from two HCVcc (*D*) independent experiments are shown. *Ab*, antibody.

HCVcc entry (39). In non-fractionated samples, blocking of SR-BI caused a marked decrease of infectivity of both HCVfrg and HCVcc samples in a dose-dependent manner (Fig. 6, *A* and *B*). Moreover, the SR-BI antibody strongly reduced infectivity of all viral subpopulations for both HCVfrg and HCVcc viruses (Fig. 6, *C* and *D*), confirming their usage of SR-BI for entry into cells.

HCVfrg Entry Depends Mostly on the Lipid Transfer Activity of SR-BI—Next, to investigate how SR-BI allows HCVfrg entry, we determined the infectivity of HCVfrg subpopulations (and of HCVcc for comparison) on Huh-7.5 cells expressing, in addition to the endogenous SR-BI, the murine ortholog mSR-BI (Fig. 7*A*), which does not bind HCV E2 (23, 47). Overexpression of either human or murine SR-BI significantly increased infectivity of both HCVcc and HCVfrg particles (Fig. 7, *C* and *D*), which indicated that SR-BI promotes HCV entry independently of E2 binding. Consistently, despite similar levels of overexpression of human and murine SR-BI (Fig. 7*A*), mSR-BI overexpression led to an augmentation of infectivity for all HCVfrg and HCVcc fractions (Fig. 7, *E* and *F*). Moreover, similarly to hSR-BI, overexpression of mSR-BI markedly increased infectivity of HCVfrg particles of very low density (<1.05 g/ml) (Fig. 7, *E* and *G*). Thus, altogether, these results highlighted the role of SR-BI for entry of *in vivo* derived particles and indicated that modulation of entry by SR-BI is independent of its capacity to bind to HCV E2.

The main physiological function of SR-BI is to transfer lipids between lipoproteins and cells (48), a function that is pivotal for HCVcc cell entry (23, 24, 47). We thus investigated the impact of the overexpression of the G420H/G424H hSR-BI mutant, which has impaired capacity to transfer lipids despite normal HDL binding capacity (49), on infectivity of HCVfrg and HCVcc subpopulations. Interestingly, we found that, despite comparable levels of cell surface expression of mutant and wild-type hSR-BI (Fig. 7, *A* and *B*), the overexpression of the G420H/G424H mutant in Huh-7.5 cells still expressing the endogenous SR-BI did not induce increased cell entry of either HCVfrg or HCVcc particles when compared with overexpression of wild-type hSR-BI regardless of their density (Fig. 7, *C*–*G*). Altogether, these results highlighted that, among the different functions of SR-BI in HCV entry, the principal factor that promotes entry of HCVfrg particles is linked to its capacity to transfer lipids.

Discussion

Many aspects of HCV biology are not completely resolved because of the lack of convenient animal models that could reproduce HCV infection and replication. An early study performed on

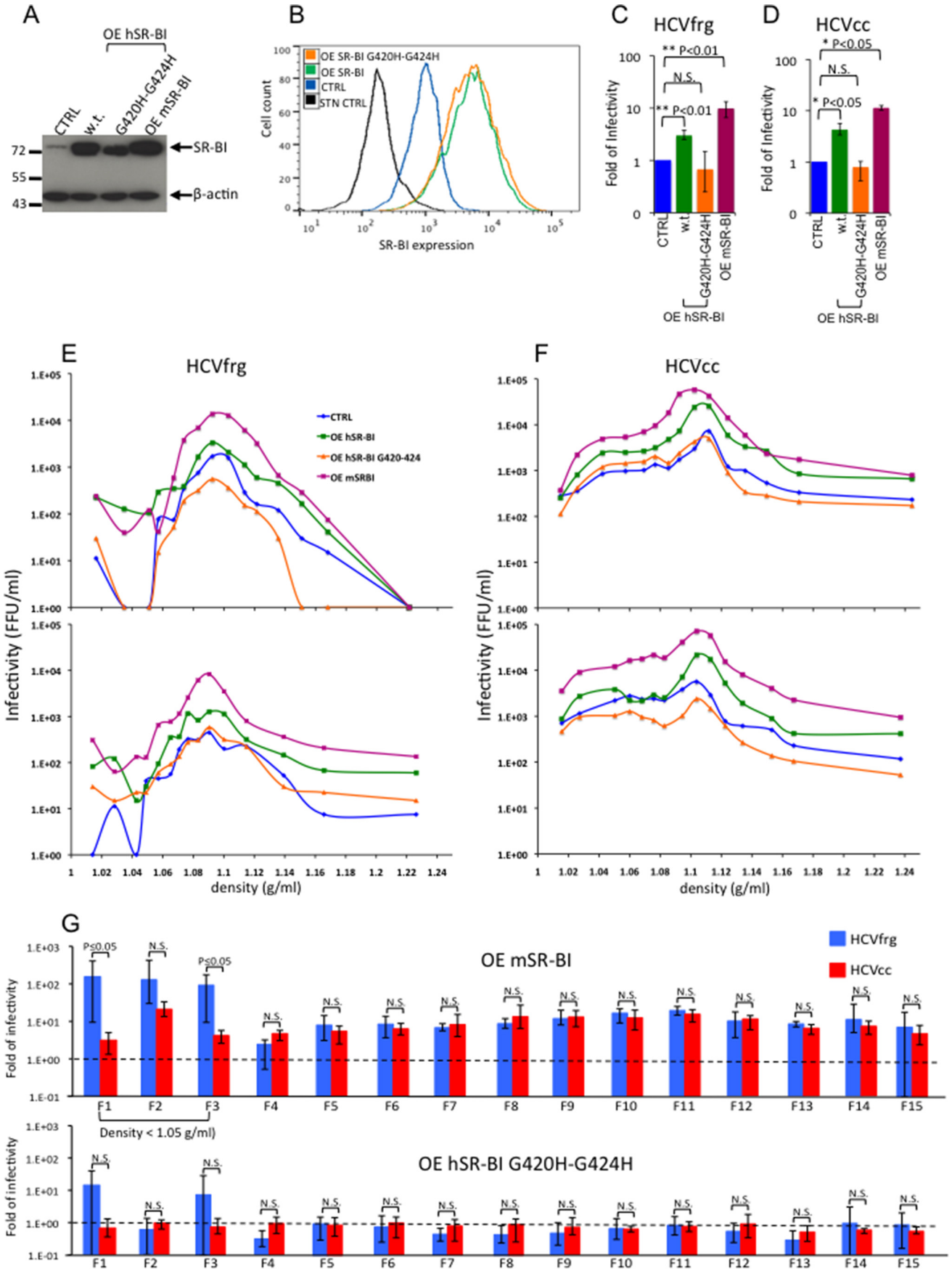

chimpanzees demonstrated that the low density viral subpopulations recovered *in vivo* were the most infectious when reinoculated in other animals (50). However, the interpretation of these results was limited by the fact that viral particles issued from chimpanzees contained anti-HCV antibodies that could have altered the intrinsic biophysical properties and infectivity of these particles. The development of immunodeficient mouse models with humanized livers that could sustain HCV infection was a great step forward to the understanding of HCV biology. Here, by using the FRG mouse model, we characterized the physicochemical and infectious properties of viral particles issued from humanized liver mice. We showed that infectious particles produced *in vivo* have a lower density compared with HCVcc particles and that a high amount of non-infectious particles with higher density circulate in the blood of these animals. Because we and others (51) have demonstrated that FRG mice have a humanized lipoprotein profile, we can speculate that the low density profile of the infectious particles is due to a different lipid and/or protein content compared with the HCVcc model.

To better characterize HCV particles issued from the FRG model, we investigated their apolipoprotein composition. Viral particle capture with apoB antibodies resulted in co-immunoprecipitation of 30% of HCVcc RNA and of less than 5% of HCVfrg RNA. The presence of apoB in viral particles issued from Huh-7.5 cells is still a matter of debate. Although some studies have indicated that apoB is dispensable for production of infectious particles (52) and is barely detected in viral particles derived from Huh-7.5 (9, 53), other studies have revealed its importance in HCV assembly and maturation (1, 11, 54). Moreover, the presence of apoB on secreted HCV particles has been demonstrated in viruses derived from cultured primary hepatocytes (32) or from long term cultures of Huh-7.5 cells differentiated with human serum-containing culture media (55) and in viruses recovered from patients (7, 8). However, in most studies, rather than direct apoB-HCV RNA co-immunoprecipitation, other methods such as affinity grid immunolabeling of apoB in precaptured tagged viruses or capture by antibody of immunoglobulin-LVP complexes followed by apoB quantification by ELISA were used (7, 8, 10). Our results using non-fractionated as well as density gradient-fractionated sera (data not shown) from infected mice suggest that HCV particles produced *in vivo* are not as accessible as HCVcc for capture with anti-apoB antibodies. As mentioned above, our co-IP experiments with HCVcc alone or mixed with sera from non-infected human liver-reconstituted FRG mice suggested that the high amount of human apoB present in the sera of these mice could compete with apoB incorporated on HCVfrg particles for the binding to the antibody. In accordance, human apoE and apoB concentrations were 2 logs higher in sera from human liver-reconstituted FRG mice as compared with supernatant from the *in vitro* HCV culture cell model (Fig. 1*C*). Moreover, we can speculate that HCVfrg particles, unlike HCVcc, are fully lipidated and that their lipid layer would mask apoB epitopes, making them inaccessible to anti-apoB antibodies. This concept is congruent with previous findings from Nielsen *et al.* (8) showing that treatment of purified LVPs in mild detergent conditions changes the apolipoprotein composition of viral particles.

In HCVfrg subpopulations, the distribution of the apoE-enriched viral particles clearly overlapped with the peak of infectivity, suggesting that this apolipoprotein plays a major role for entry of *in vivo* derived particles. On the contrary, for HCVcc particles, apoE co-immunoprecipitated with HCV RNA in all fractions irrespective of their infectious properties, indicating that a high proportion of apoE-containing particles issued from *in vitro* cultures are poorly infectious. This could reflect an improper maturation of lipoproteins (and thus of viral particles) in Huh-7.5 cells (30), which would not allow a correct incorporation and/or folding of apolipoproteins into lipoproteins and thus HCV particles. Alternatively, we could surmise that the physicochemical composition of HCVfrg particles retrieved from peripheral blood could be modified by peripheral lipoprotein lipases that influence VLDL lipid and apolipoprotein composition. Indeed, Shimizu *et al.* (56) showed that lipoprotein lipase treatment of HCVcc particles resulted in a decreased infectivity, a shift toward higher density, and a loss of apoE in viral particles. Finally and in a more general way, it has been demonstrated that in recombinant HDL complexes the lipid content modulates the stability of apoA-I (57), which indicates that lipid content modifications influence the apolipoprotein composition of lipoproteins. Thus, modifications of the lipid content of viral particles may influence the stability of their apolipoproteins.

HCV entry is a complex mechanism involving multiple cellular receptors. In a previous work, we demonstrated that among them SR-BI modulates entry of HCVcc subpopulations depending on their physicochemical properties (23). Because the initial capture of intermediate density HCVcc particles involves binding of SR-BI to apoE incorporated on viral particles and because we have observed a different distribution of this apolipoprotein in HCVfrg *versus* HCVcc subpopulations, we investigated the reliance on SR-BI for entry of HCVfrg subpopulations. First, we show that HCV particles recovered from sera of infected mice are dependent on SR-BI for entry because its down- or up-regulation modulated infectivity by about 1 log compared with control cells. These data are in accordance with Grove *et al.* (58) who showed that SR-BI up-regulation

FIGURE 7. **HCVfrg and HCVcc particles exploit different SR-BI properties for entry depending on the biophysical and cellular determinants of the viral particles.** *A*, Western blot analysis of Huh-7.5 cells overexpressing mouse SR-BI (*OE mSR-BI*), human SR-BI (*OE hSR-BI*), or the mutant form of hSR-BI (*OE hSR-BI G420H-G424H*) or non-transduced cells as a control. Cell lysates were stained with anti-SR-BI antibody and with anti-β-actin antibody (AC74, Sigma). *B*, flow cytometry analysis of Huh-7.5 cells overexpressing (*OE*) the wild type or the G420H/G424H hSR-BI mutant (*OE hSR-BI G420H-G424H*). *CTRL*, cells transduced with the backbone vector expressing the GFP; *STN CTRL*, staining without the primary antibody. Huh-7.5 cells overexpressing human SR-BI (*OE hSR-BI*), mouse SR-BI (*OE mSR-BI*), or G420H/G424H hSR-BI mutant (*OE hSR-BI G420H-G424H*) were infected with non-fractionated HCVfrg (*C*; $n = 5$) or HCVcc (*D*; $n = 3$) or with serial dilutions of the gradient density-separated fractions of HCVfrg (*E*) or HCVcc (*F*). Infectivity was calculated for equivalent volumes for each fraction. Note that up-regulated cells and controls express the endogenous SR-BI. Statistical analyses were performed on total infectivity with Student's *t* test. *N.S.*, not statistically significant. *G*, -fold increase of infectivity of HCVfrg and HCVcc subpopulations in mSR-BI- or hSR-BI G420H/G424H-overexpressing cells compared with the controls. Results are the average of four HCVfrg and four HCVcc independent experiments and are shown for each density fraction (*F1–F15*). Statistical analyses were performed by a Mann-Whitney test. *N.S.*, not statistically significant. *Error bars* represent S.D.

increased by 4-fold the infectivity of sera from HCV-infected humanized liver uPA/SCID mice.

Importantly, the expression of the murine SR-BI ortholog, which does not bind HCV E2 (23, 47), resulted in an augmentation of infectivity in all of the HCVfrg subpopulations, demonstrating that modulation of entry by SR-BI is independent of its capacity to bind HCV E2. The expression of the murine SR-BI ortholog resulted in a greater increase of infectivity of both HCVfrg and HCVcc particles compared with the overexpression of human SR-BI. We suggest that, despite the expression of an equivalent amount of mouse and human SR-BI in transduced cells as shown by Western blot analysis (Fig. 7*A*), mSR-BI could be preferentially expressed at the membrane surface in Huh-7.5 cells or alternatively that the internalization rate of the virus-receptor complexes could be different for the human *versus* murine SR-BI. Overall, the expression, stability, localization, and interaction with other receptors and factors that promote HCV entry of mSR-BI or hSR-BI could be differentially regulated.

Moreover, we show that entry of HCVfrg particles pertains to the lipid transfer activity of SR-BI, and our data underscore that this is a feature required independently of the density of the particle subpopulations. Thus, our study highlights that entry of *in vivo* produced HCV particles is strictly dependent on the physiological functions of SR-BI and likely on the incorporated lipoprotein components rather than on the capacity of this receptor to bind viral surface glycoproteins.

We found that SR-BI expression is a limiting factor for entry of the most infectious particles for both HCVfrg and HCVcc models (*i.e.* of intermediate-high density, 1.06–1.11 and 1.08–1.14 g/ml, respectively). This observation is consistent with previous findings that HDLs, which have a density of >1.06 g/ml, are natural ligands of SR-BI that facilitate HCV entry (25). Within these subpopulations, the increase of infectivity in HCVcc was significantly higher than in HCVfrg subpopulations. Because we had previously demonstrated that in these subpopulations SR-BI-mediated entry depends on its interplay with E2 (23), we can speculate that in HCVcc particles the viral glycoproteins are more accessible for the binding to SR-BI as compared with HCVfrg particles. Alternatively, because HDL-mediated entry enhancement is regulated by E2 (23) and because the available HDL amounts are likely different for HCVfrg sera and HCVcc supernatants, such variations might exacerbate distinct dependence on SR-BI. In accordance, in cells overexpressing mSR-BI, which does not bind E2, there was no difference in the increase of infectivity between HCVfrg and HCVcc of intermediate-high densities.

However, these subpopulations are dependent on SR-BI levels to a lower extent as compared with the low density HCVfrg subpopulations. Indeed, strikingly, we demonstrate that HCVfrg subpopulations have a non-homogeneous reliance on SR-BI expression levels for entry. Especially, SR-BI overexpression revealed that entry of the very low density populations (*i.e.* <1.05 g/ml) are the most dependent on the level of SR-BI expression because its overexpression increased infectivity by at least 10–100-fold as compared with the HCV particles of alternative densities (*i.e.* up to 10-fold). SR-BI is a natural receptor for HDL but also for native LDL, oxidized LDL, and VLDL (48). Because we showed that SR-BI-mediated HCVfrg entry is independent of its capacity to bind E2 and because we and others have found that SR-BI likely interacts with HCV particles via lipoprotein components (23, 42, 43), we can argue that in low density HCVfrg populations (*i.e.* <1.05 g/ml, which corresponds to the superior limit of LDL density), the high amount of serum LDL competed with HCV for SR-BI binding. Thus, increasing the SR-BI expression level would improve binding of low density HCVfrg populations. This assumption is congruent with a previous demonstration that the interaction between serum-derived HCV and SR-BI was competed out by VLDL (59). Alternatively, SR-BI overexpression may prevent, at least partially, binding of viral particles to LDL receptor, which has been demonstrated to be a receptor conducive to a "non-productive" infection (60). In contrast, in the HCVcc model, SR-BI expression is not differentially limiting for entry of low density viral particles perhaps because the concentration of lipoproteins in the supernatant of hepatoma cell lines is lower as depicted by lower levels of the representative components apoE and apoB (Fig. 1*C*) compared with the serum of infected mice. Indeed, statistical analyses highlighted a significant increase of infectivity in HCVfrg low density populations (*i.e.* <1.05 g/ml) upon SR-BI upregulation compared with HCVcc low density populations. The levels of SR-BI expression in the liver are known to vary upon various stimulations, including the quantity and nature of intracellular lipids (61) and external stimulation by dietary compounds such as lipids or fibrates (62–64). Such variations might have a great impact on viral entry and spread, especially for the low density virus because of its potentially high specific infectivity *in vivo* and its resistance to neutralization by antibodies (50).

In conclusion, our results highlight previously uncharacterized divergences between *in vivo* and *in vitro* produced HCV particles with respect to their composition and biophysical properties, which imprint their infectivity and receptor usage. Thus, humanized liver mouse models represent a powerful tool to investigate the interplay between HCV and liver components and to understand how the hepatic environment influences HCV biology.

Author Contributions—S. C., M. D., and F.-L. C. coordinated the project, designed experiments, analyzed the data, and wrote the manuscript. S. C., F. F., J. M., V. L. D. T., N. G., and C. G. designed and performed experiments and analyzed the data. J.-Y. S. and D. L. provided critical discussion and technical advice. M. B. Z. and T. F. B. provided critical reagents and analyzed the data.

Acknowledgments—We are grateful to M. Grompe for providing FRG mice, C. Rice for the Huh-7.5 cell line and the NS5A monoclonal antibody, and M. Law for providing the AR3A antibody. We thank J. F. Henry, N. Aguilera, and J. L. Thoumas from the animal facility (Plateau de Biologie Experimental de la Souris, Structure Fédérative de Recherche (SFR) Biosciences, École Normale Supérieure (ENS) de Lyon) as well as G. Froment from the UMS3444/US8, SFR Biosciences for technical help in handling mice. We thank A. Geloen from Institut National de Sciences Appliquées de Lyon for help in performing lipoprotein assays. We thank C. Chamot from the microscopy facility (Plateau Technique Imagerie/Microscopie, SFR Biosciences, ENS de Lyon) for assistance in setting up the ImageJ macro program. We thank the vectorology platform (INSERM U1089, Nantes, France) for the production of the Adeno-uPA vector.

References

1. Huang, H., Sun, F., Owen, D. M., Li, W., Chen, Y., Gale, M., Jr., and Ye, J. (2007) Hepatitis C virus production by human hepatocytes dependent on assembly and secretion of very low-density lipoproteins. *Proc. Natl. Acad. Sci. U.S.A.* **104,** 5848–5853
2. Bartenschlager, R., Penin, F., Lohmann, V., and André, P. (2011) Assembly of infectious hepatitis C virus particles. *Trends Microbiol.* **19,** 95–103
3. Sundaram, M., and Yao, Z. (2012) Intrahepatic role of exchangeable apolipoproteins in lipoprotein assembly and secretion. *Arterioscler. Thromb. Vasc. Biol.* **32,** 1073–1078
4. Thomssen, R., Bonk, S., Propfe, C., Heermann, K. H., Köchel, H. G., and Uy, A. (1992) Association of hepatitis C virus in human sera with β-lipoprotein. *Med. Microbiol. Immunol.* **181,** 293–300
5. Thomssen, R., Bonk, S., and Thiele, A. (1993) Density heterogeneities of hepatitis C virus in human sera due to the binding of β-lipoproteins and immunoglobulins. *Med. Microbiol. Immunol.* **182,** 329–334
6. Hijikata, M., Shimizu, Y. K., Kato, H., Iwamoto, A., Shih, J. W., Alter, H. J., Purcell, R. H., and Yoshikura, H. (1993) Equilibrium centrifugation studies of hepatitis C virus: evidence for circulating immune complexes. *J. Virol.* **67,** 1953–1958
7. André, P., Komurian-Pradel, F., Deforges, S., Perret, M., Berland, J. L., Sodoyer, M., Pol, S., Bréchot, C., Paranhos-Baccalà, G., and Lotteau, V. (2002) Characterization of low- and very-low-density hepatitis C virus RNA-containing particles. *J. Virol.* **76,** 6919–6928
8. Nielsen, S. U., Bassendine, M. F., Burt, A. D., Martin, C., Pumeechockchai, W., and Toms, G. L. (2006) Association between hepatitis C virus and very-low-density lipoprotein (VLDL)/LDL analyzed in iodixanol density gradients. *J. Virol.* **80,** 2418–2428
9. Merz, A., Long, G., Hiet, M. S., Brügger, B., Chlanda, P., Andre, P., Wieland, F., Krijnse-Locker, J., and Bartenschlager, R. (2011) Biochemical and morphological properties of hepatitis C virus particles and determination of their lipidome. *J. Biol. Chem.* **286,** 3018–3032
10. Catanese, M. T., Uryu, K., Kopp, M., Edwards, T. J., Andrus, L., Rice, W. J., Silvestry, M., Kuhn, R. J., and Rice, C. M. (2013) Ultrastructural analysis of hepatitis C virus particles. *Proc. Natl. Acad. Sci. U.S.A.* **110,** 9505–9510
11. Boyer, A., Dumans, A., Beaumont, E., Etienne, L., Roingeard, P., and Meunier, J. C. (2014) The association of hepatitis C virus glycoproteins with apolipoproteins e and B early in assembly is conserved in lipoviral particles. *J. Biol. Chem.* **289,** 18904–18913
12. Lee, J. Y., Acosta, E. G., Stoeck, I. K., Long, G., Hiet, M. S., Mueller, B., Fackler, O. T., Kallis, S., and Bartenschlager, R. (2014) Apolipoprotein E likely contributes to a maturation step of infectious hepatitis C virus particles and interacts with viral envelope glycoproteins. *J. Virol.* **88,** 12422–12437
13. Fukuhara, T., Wada, M., Nakamura, S., Ono, C., Shiokawa, M., Yamamoto, S., Motomura, T., Okamoto, T., Okuzaki, D., Yamamoto, M., Saito, I., Wakita, T., Koike, K., and Matsuura, Y. (2014) Amphipathic α-helices in apolipoproteins are crucial to the formation of infectious hepatitis C virus particles. *PLoS Pathog.* **10,** e1004534
14. Barth, H., Schafer, C., Adah, M. I., Zhang, F., Linhardt, R. J., Toyoda, H., Kinoshita-Toyoda, A., Toida, T., Van Kuppevelt, T. H., Depla, E., Von Weizsacker, F., Blum, H. E., and Baumert, T. F. (2003) Cellular binding of hepatitis C virus envelope glycoprotein E2 requires cell surface heparan sulfate. *J. Biol. Chem.* **278,** 41003–41012
15. Agnello, V., Abel, G., Elfahal, M., Knight, G. B., and Zhang, Q. X. (1999) Hepatitis C virus and other Flaviviridae viruses enter cells via low density lipoprotein receptor. *Proc. Natl. Acad. Sci. U.S.A.* **96,** 12766–12771
16. Scarselli, E., Ansuini, H., Cerino, R., Roccasecca, R. M., Acali, S., Filocamo, G., Traboni, C., Nicosia, A., Cortese, R., and Vitelli, A. (2002) The human scavenger receptor class B type I is a novel candidate receptor for the hepatitis C virus. *EMBO J.* **21,** 5017–5025
17. Pileri, P., Uematsu, Y., Campagnoli, S., Galli, G., Falugi, F., Petracca, R., Weiner, A. J., Houghton, M., Rosa, D., Grandi, G., and Abrignani, S. (1998) Binding of hepatitis C virus to CD81. *Science* **282,** 938–941
18. Evans, M. J., von Hahn, T., Tscherne, D. M., Syder, A. J., Panis, M., Wölk, B., Hatziioannou, T., McKeating, J. A., Bieniasz, P. D., and Rice, C. M. (2007) Claudin-1 is a hepatitis C virus co-receptor required for a late step in entry. *Nature* **446,** 801–805
19. Ploss, A., Evans, M. J., Gaysinskaya, V. A., Panis, M., You, H., de Jong, Y. P., and Rice, C. M. (2009) Human occludin is a hepatitis C virus entry factor required for infection of mouse cells. *Nature* **457,** 882–886
20. Blanchard, E., Belouzard, S., Goueslain, L., Wakita, T., Dubuisson, J., Wychowski, C., and Rouillé, Y. (2006) Hepatitis C virus entry depends on clathrin-mediated endocytosis. *J. Virol.* **80,** 6964–6972
21. Sainz, B., Jr., Barretto, N., Martin, D. N., Hiraga, N., Imamura, M., Hussain, S., Marsh, K. A., Yu, X., Chayama, K., Alrefai, W. A., and Uprichard, S. L. (2012) Identification of the Niemann-Pick C1-like 1 cholesterol absorption receptor as a new hepatitis C virus entry factor. *Nat. Med.* **18,** 281–285
22. Lupberger, J., Zeisel, M. B., Xiao, F., Thumann, C., Fofana, I., Zona, L., Davis, C., Mee, C. J., Turek, M., Gorke, S., Royer, C., Fischer, B., Zahid, M. N., Lavillette, D., Fresquet, J., Cosset, F. L., Rothenberg, S. M., Pietschmann, T., Patel, A. H., Pessaux, P., Doffoël, M., Raffelsberger, W., Poch, O., McKeating, J. A., Brino, L., and Baumert, T. F. (2011) EGFR and EphA2 are host factors for hepatitis C virus entry and possible targets for antiviral therapy. *Nat. Med.* **17,** 589–595
23. Dao Thi, V. L., Granier, C., Zeisel, M. B., Guérin, M., Mancip, J., Granio, O., Penin, F., Lavillette, D., Bartenschlager, R., Baumert, T. F., Cosset, F. L., and Dreux, M. (2012) Characterization of hepatitis C virus particle subpopulations reveals multiple usage of the scavenger receptor BI for entry steps. *J. Biol. Chem.* **287,** 31242–31257
24. Dreux, M., Dao Thi, V. L., Fresquet, J., Guérin, M., Julia, Z., Verney, G., Durantel, D., Zoulim, F., Lavillette, D., Cosset, F. L., and Bartosch, B. (2009) Receptor complementation and mutagenesis reveal SR-BI as an essential HCV entry factor and functionally imply its intra- and extracellular domains. *PLoS Pathog.* **5,** e1000310
25. Bartosch, B., Verney, G., Dreux, M., Donot, P., Morice, Y., Penin, F., Pawlotsky, J. M., Lavillette, D., and Cosset, F. L. (2005) An interplay between hypervariable region 1 of the hepatitis C virus E2 glycoprotein, the scavenger receptor BI, and high-density lipoprotein promotes both enhancement of infection and protection against neutralizing antibodies. *J. Virol.* **79,** 8217–8229
26. Lindenbach, B. D., Evans, M. J., Syder, A. J., Wölk, B., Tellinghuisen, T. L., Liu, C. C., Maruyama, T., Hynes, R. O., Burton, D. R., McKeating, J. A., and Rice, C. M. (2005) Complete replication of hepatitis C virus in cell culture. *Science* **309,** 623–626
27. Wakita, T., Pietschmann, T., Kato, T., Date, T., Miyamoto, M., Zhao, Z., Murthy, K., Habermann, A., Kräusslich, H. G., Mizokami, M., Bartenschlager, R., and Liang, T. J. (2005) Production of infectious hepatitis C virus in tissue culture from a cloned viral genome. *Nat. Med.* **11,** 791–796
28. Zhong, J., Gastaminza, P., Cheng, G., Kapadia, S., Kato, T., Burton, D. R., Wieland, S. F., Uprichard, S. L., Wakita, T., and Chisari, F. V. (2005) Robust hepatitis C virus infection *in vitro*. *Proc. Natl. Acad. Sci. U.S.A.* **102,** 9294–9299
29. Pietschmann, T., Kaul, A., Koutsoudakis, G., Shavinskaya, A., Kallis, S., Steinmann, E., Abid, K., Negro, F., Dreux, M., Cosset, F. L., and Bartenschlager, R. (2006) Construction and characterization of infectious intragenotypic and intergenotypic hepatitis C virus chimeras. *Proc. Natl. Acad. Sci. U.S.A.* **103,** 7408–7413
30. Meex, S. J., Andreo, U., Sparks, J. D., and Fisher, E. A. (2011) Huh-7 or HepG2 cells: which is the better model for studying human apolipoprotein-B100 assembly and secretion? *J. Lipid Res.* **52,** 152–158
31. Lindenbach, B. D., Meuleman, P., Ploss, A., Vanwolleghem, T., Syder, A. J., McKeating, J. A., Lanford, R. E., Feinstone, S. M., Major, M. E., Leroux-Roels, G., and Rice, C. M. (2006) Cell culture-grown hepatitis C virus is infectious *in vivo* and can be recultured *in vitro*. *Proc. Natl. Acad. Sci. U.S.A.* **103,** 3805–3809
32. Podevin, P., Carpentier, A., Pène, V., Aoudjehane, L., Carrière, M., Zaïdi, S., Hernandez, C., Calle, V., Méritet, J. F., Scatton, O., Dreux, M., Cosset, F. L., Wakita, T., Bartenschlager, R., Demignot, S., Conti, F., Rosenberg, A. R., and Calmus, Y. (2010) Production of infectious hepatitis C virus in primary cultures of human adult hepatocytes. *Gastroenterology* **139,** 1355–1364
33. Mercer, D. F., Schiller, D. E., Elliott, J. F., Douglas, D. N., Hao, C., Rinfret, A., Addison, W. R., Fischer, K. P., Churchill, T. A., Lakey, J. R., Tyrrell,

D. L., and Kneteman, N. M. (2001) Hepatitis C virus replication in mice with chimeric human livers. *Nat. Med.* **7,** 927–933
34. Bissig, K. D., Le, T. T., Woods, N. B., and Verma, I. M. (2007) Repopulation of adult and neonatal mice with human hepatocytes: a chimeric animal model. *Proc. Natl. Acad. Sci. U.S.A.* **104,** 20507–20511
35. Azuma, H., Paulk, N., Ranade, A., Dorrell, C., Al-Dhalimy, M., Ellis, E., Strom, S., Kay, M. A., Finegold, M., and Grompe, M. (2007) Robust expansion of human hepatocytes in Fah−/−/Rag2−/−/Il2rg−/− mice. *Nat. Biotechnol.* **25,** 903–910
36. Bissig, K. D., Wieland, S. F., Tran, P., Isogawa, M., Le, T. T., Chisari, F. V., and Verma, I. M. (2010) Human liver chimeric mice provide a model for hepatitis B and C virus infection and treatment. *J. Clin. Investig.* **120,** 924–930
37. Boson, B., Granio, O., Bartenschlager, R., and Cosset, F. L. (2011) A concerted action of hepatitis C virus p7 and nonstructural protein 2 regulates core localization at the endoplasmic reticulum and virus assembly. *PLoS Pathog.* **7,** e1002144
38. Lavillette, D., Tarr, A. W., Voisset, C., Donot, P., Bartosch, B., Bain, C., Patel, A. H., Dubuisson, J., Ball, J. K., and Cosset, F. L. (2005) Characterization of host-range and cell entry properties of the major genotypes and subtypes of hepatitis C virus. *Hepatology* **41,** 265–274
39. Zahid, M. N., Turek, M., Xiao, F., Thi, V. L., Guérin, M., Fofana, I., Bachellier, P., Thompson, J., Delang, L., Neyts, J., Bankwitz, D., Pietschmann, T., Dreux, M., Cosset, F. L., Grunert, F., Baumert, T. F., and Zeisel, M. B. (2013) The postbinding activity of scavenger receptor class B type I mediates initiation of hepatitis C virus infection and viral dissemination. *Hepatology* **57,** 492–504
40. Law, M., Maruyama, T., Lewis, J., Giang, E., Tarr, A. W., Stamataki, Z., Gastaminza, P., Chisari, F. V., Jones, I. M., Fox, R. I., Ball, J. K., McKeating, J. A., Kneteman, N. M., and Burton, D. R. (2008) Broadly neutralizing antibodies protect against hepatitis C virus quasispecies challenge. *Nat. Med.* **14,** 25–27
41. Lavillette, D., Morice, Y., Germanidis, G., Donot, P., Soulier, A., Pagkalos, E., Sakellariou, G., Intrator, L., Bartosch, B., Pawlotsky, J. M., and Cosset, F. L. (2005) Human serum facilitates hepatitis C virus infection, and neutralizing responses inversely correlate with viral replication kinetics at the acute phase of hepatitis C virus infection. *J. Virol.* **79,** 6023–6034
42. Jiang, J., Cun, W., Wu, X., Shi, Q., Tang, H., and Luo, G. (2012) Hepatitis C virus attachment mediated by apolipoprotein E binding to cell surface heparan sulfate. *J. Virol.* **86,** 7256–7267
43. Lefèvre, M., Felmlee, D. J., Parnot, M., Baumert, T. F., and Schuster, C. (2014) Syndecan 4 is involved in mediating HCV entry through interaction with lipoviral particle-associated apolipoprotein E. *PLoS One* **9,** e95550
44. Xu, Y., Martinez, P., Séron, K., Luo, G., Allain, F., Dubuisson, J., and Belouzard, S. (2015) Characterization of hepatitis C virus interaction with heparan sulfate proteoglycans. *J. Virol* **89,** 3846–3858
45. Hueging, K., Doepke, M., Vieyres, G., Bankwitz, D., Frentzen, A., Doerrbecker, J., Gumz, F., Haid, S., Wölk, B., Kaderali, L., and Pietschmann, T. (2014) Apolipoprotein E codetermines tissue tropism of hepatitis C virus and is crucial for viral cell-to-cell transmission by contributing to a postenvelopment step of assembly. *J. Virol.* **88,** 1433–1446
46. Jiang, J., Wu, X., Tang, H., and Luo, G. (2013) Apolipoprotein E mediates attachment of clinical hepatitis C virus to hepatocytes by binding to cell surface heparan sulfate proteoglycan receptors. *PLoS One* **8,** e67982
47. Catanese, M. T., Ansuini, H., Graziani, R., Huby, T., Moreau, M., Ball, J. K., Paonessa, G., Rice, C. M., Cortese, R., Vitelli, A., and Nicosia, A. (2010) Role of scavenger receptor class B type I in hepatitis C virus entry: kinetics and molecular determinants. *J. Virol.* **84,** 34–43
48. Rhainds, D., and Brissette, L. (2004) The role of scavenger receptor class B type I (SR-BI) in lipid trafficking. Defining the rules for lipid traders. *Int. J. Biochem. Cell Biol.* **36,** 39–77
49. Parathath, S., Sahoo, D., Darlington, Y. F., Peng, Y., Collins, H. L., Rothblat, G. H., Williams, D. L., and Connelly, M. A. (2004) Glycine 420 near the C-terminal transmembrane domain of SR-BI is critical for proper delivery and metabolism of high density lipoprotein cholesteryl ester. *J. Biol. Chem.* **279,** 24976–24985
50. Bradley, D., McCaustland, K., Krawczynski, K., Spelbring, J., Humphrey, C., and Cook, E. H. (1991) Hepatitis C virus: buoyant density of the factor VIII-derived isolate in sucrose. *J. Med. Virol.* **34,** 206–208
51. Ellis, E. C., Naugler, W. E., Nauglers, S., Parini, P., Mörk, L. M., Jorns, C., Zemack, H., Sandblom, A. L., Björkhem, I., Ericzon, B. G., Wilson, E. M., Strom, S. C., and Grompe, M. (2013) Mice with chimeric livers are an improved model for human lipoprotein metabolism. *PLoS One* **8,** e78550
52. Jiang, J., and Luo, G. (2009) Apolipoprotein E but not B is required for the formation of infectious hepatitis C virus particles. *J. Virol.* **83,** 12680–12691
53. Jammart, B., Michelet, M., Pécheur, E. I., Parent, R., Bartosch, B., Zoulim, F., and Durantel, D. (2013) Very-low-density lipoprotein (VLDL)-producing and hepatitis C virus-replicating HepG2 cells secrete no more lipoviroparticles than VLDL-deficient Huh7.5 cells. *J. Virol.* **87,** 5065–5080
54. Gastaminza, P., Cheng, G., Wieland, S., Zhong, J., Liao, W., and Chisari, F. V. (2008) Cellular determinants of hepatitis C virus assembly, maturation, degradation, and secretion. *J. Virol.* **82,** 2120–2129
55. Steenbergen, R. H., Joyce, M. A., Thomas, B. S., Jones, D., Law, J., Russell, R., Houghton, M., and Tyrrell, D. L. (2013) Human serum leads to differentiation of human hepatoma cells, restoration of very-low-density lipoprotein secretion, and a 1000-fold increase in HCV Japanese fulminant hepatitis type 1 titers. *Hepatology* **58,** 1907–1917
56. Shimizu, Y., Hishiki, T., Sugiyama, K., Ogawa, K., Funami, K., Kato, A., Ohsaki, Y., Fujimoto, T., Takaku, H., and Shimotohno, K. (2010) Lipoprotein lipase and hepatic triglyceride lipase reduce the infectivity of hepatitis C virus (HCV) through their catalytic activities on HCV-associated lipoproteins. *Virology* **407,** 152–159
57. Sparks, D. L., Davidson, W. S., Lund-Katz, S., and Phillips, M. C. (1995) Effects of the neutral lipid content of high density lipoprotein on apolipoprotein A-I structure and particle stability. *J. Biol. Chem.* **270,** 26910–26917
58. Grove, J., Huby, T., Stamataki, Z., Vanwolleghem, T., Meuleman, P., Farquhar, M., Schwarz, A., Moreau, M., Owen, J. S., Leroux-Roels, G., Balfe, P., and McKeating, J. A. (2007) Scavenger receptor BI and BII expression levels modulate hepatitis C virus infectivity. *J. Virol.* **81,** 3162–3169
59. Maillard, P., Huby, T., Andréo, U., Moreau, M., Chapman, J., and Budkowska, A. (2006) The interaction of natural hepatitis C virus with human scavenger receptor SR-BI/Cla1 is mediated by apoB-containing lipoproteins. *FASEB J.* **20,** 735–737
60. Albecka, A., Belouzard, S., Op de Beeck, A., Descamps, V., Goueslain, L., Bertrand-Michel, J., Tercé, F., Duverlie, G., Rouillé, Y., and Dubuisson, J. (2012) Role of low-density lipoprotein receptor in the hepatitis C virus life cycle. *Hepatology* **55,** 998–1007
61. Li, G., Thomas, A. M., Williams, J. A., Kong, B., Liu, J., Inaba, Y., Xie, W., and Guo, G. L. (2012) Farnesoid X receptor induces murine scavenger receptor Class B type I via intron binding. *PLoS One* **7,** e35895
62. Spady, D. K., Kearney, D. M., and Hobbs, H. H. (1999) Polyunsaturated fatty acids up-regulate hepatic scavenger receptor B1 (SR-BI) expression and HDL cholesteryl ester uptake in the hamster. *J. Lipid Res.* **40,** 1384–1394
63. Loison, C., Mendy, F., Sérougne, C., and Lutton, C. (2002) Dietary myristic acid modifies the HDL-cholesterol concentration and liver scavenger receptor BI expression in the hamster. *Br. J. Nutr.* **87,** 199–210
64. Mardones, P., Pilon, A., Bouly, M., Duran, D., Nishimoto, T., Arai, H., Kozarsky, K. F., Altayo, M., Miquel, J. F., Luc, G., Clavey, V., Staels, B., and Rigotti, A. (2003) Fibrates down-regulate hepatic scavenger receptor class B type I protein expression in mice. *J. Biol. Chem.* **278,** 7884–7890
65. de Jong, Y. P., Dorner, M., Mommersteeg, M. C., Xiao, J. W., Balazs, A. B., Robbins, J. B., Winer, B. Y., Gerges, S., Vega, K., Labitt, R. N., Donovan, B. M., Giang, E., Krishnan, A., Chiriboga, L., Charlton, M. R., Burton, D. R., Baltimore, D., Law, M., Rice, C. M., and Ploss, A. (2014) Broadly neutralizing antibodies abrogate established hepatitis C virus infection. *Sci. Transl. Med.* **6,** 254ra129

Functional and Biochemical Characterization of Hepatitis C Virus (HCV) Particles Produced in a Humanized Liver Mouse Model

Sara Calattini, Floriane Fusil, Jimmy Mancip, Viet Loan Dao Thi, Christelle Granier, Nicolas Gadot, Jean-Yves Scoazec, Mirjam B. Zeisel, Thomas F. Baumert, Dimitri Lavillette, Marlène Dreux and François-Loïc Cosset

J. Biol. Chem. 2015, 290:23173-23187.
doi: 10.1074/jbc.M115.662999 originally published online July 29, 2015
